Compound FC-10696 Inhibits Egress and Spread of Marburg Virus

Ziying Han[1], Hong Ye[2], Jingjing Liang[1], Ariel Shepley-McTaggart[1], Jay E. Wrobel[2], Allen B. Reitz[2], Alison Whigham[4], Katrina N. Kavelish[4], Michael S. Saporito[3], Bruce D. Freedman[1], Olena Shtanko[4]*, and Ronald N. Harty[1]*

[1]University of Pennsylvania, Philadelphia, Pennsylvania, USA; [2]Fox Chase Chemical Diversity Center, Doylestown, Pennsylvania, USA; [3]Intervir, LLC, Philadelphia, Pennsylvania, USA; [4]Texas Biomedical Research Institute, San Antonio, Texas, USA.

***Co-Corresponding Authors**: Dr. Ronald N. Harty, Professor, Department of Pathobiology, School of Veterinary Medicine, University of Pennsylvania, 3800 Spruce Street, Philadelphia, PA 19104, USA. Phone: 215-573-4485, Fax: 215-898-7887, Email: rharty@vet.upenn.edu; Dr. Olena Shtanko, Texas Biomedical Research Institute, San Antonio, TX 78227, USA. Phone: 210-258-9400, Email: oshtanko@txbiomed.org.

Running Title: Host-Oriented Inhibition of MARV Egress.

Key Words: Marburg virus, filovirus, PPxY motif, L-domain, antiviral therapeutic, host-oriented, budding, WW-domain, Nedd4, virus-host interaction

Abstract: Marburg virus (MARV) VP40 protein (mVP40) directs egress and spread of MARV, in part, by recruiting specific host WW-domain containing proteins via its conserved PPxY Late (L) domain motif to facilitate efficient virus-cell separation. We reported previously that small molecule compounds targeting the viral PPxY/host WW-domain interaction inhibited VP40-mediated egress and spread. Here, we report on the antiviral potency of novel compound FC-10696, which emerged from extensive structure activity relationship (SAR) of a previously described series of PPxY inhibitors. We show that FC-10696 inhibits egress of both mVP40 VLPs and egress and spread of authentic MARV from HeLa cells and primary human macrophages. Moreover, FC-10696 treated mice displayed delayed onset of weight loss, clinical signs, and significantly lower viral loads compared to controls, with 14% of animals surviving 21 days following a lethal MARV challenge. Thus, FC-10696 represents a first-in-class, host-oriented inhibitor effectively targeting late stages of the MARV lifecycle.

Introduction: MARV is an emerging pathogen and potential bioterror agent that can cause severe hemorrhagic fever in humans and non-human primates (1). Currently, there are no approved vaccines or antiviral therapeutics to prevent or treat MARV infections. Development of novel and effective antiviral therapeutics against MARV and other members of the *Filoviridae* family are urgently needed.

MARV, like many other enveloped RNA viruses, relies on its matrix protein (mVP40) to direct and promote budding of infectious virions. We and others have demonstrated that mVP40 completes the budding process, in part, by using its highly conserved PPxY L-domain motif to hijack host proteins/pathways that then facilitate efficient virus-cell separation (2-16). One of the best characterized host interactors is WW-domain containing E3 ubiquitin ligase, Nedd4 (7, 16-18). Notably, we and others have shown that Nedd4 and Nedd4 family members physically interact with viral PPxY motifs via one or more of their WW-domains, and functionally interact with viral PPxY-containing proteins to enhance or promote budding of virus-like particles (VLPs) and live virus (7, 16-24). The highly conserved physical and functional nature of the PPxY motif in a wide array of RNA viruses, makes it an attractive target for the development of antivirals (2, 25-30). Indeed, compounds targeting the PPxY/WW-domain virus-host interaction would be predicted to dampen or reduce the ability of the virus to bud or pinch-off from infected cells, thus allowing an individual's immune system more time to combat and clear the virus.

Previously, we described the identification and development of two novel series of small molecule compounds that significantly inhibited a VP40-Nedd4 interaction and PPxY-mediated egress of filovirus VP40 VLPs (26). We went on to show that our lead compounds significantly inhibited budding of a live VSV recombinant (VSV-M40) that we engineered to express the PPxY motif from Ebola virus (EBOV) VP40 in place of that from the VSV matrix (M) protein (26). Following extensive SAR and analog testing, we have now identified lead compound FC-10696, which we have shown is stable in human liver microsomes and possesses suitable ADME and PK properties for IP administration and testing in mice. Indeed, here we show that nanomolar concentrations of FC-10696 blocked budding of mVP40 VLPs. Moreover, we demonstrate that similar concentrations of FC-10696 also significantly inhibited egress and

spread of live MARV in both HeLa cells and human monocyte derived macrophages (hMDM) with little to no cytotoxicity at the effective antiviral concentrations. Importantly, we show proof-of-concept *in vivo* efficacy of FC-10696 in a mouse challenge model of MARV disease. Indeed, FC-10696-treated animals exhibited delayed onset of weight loss, clinical signs, and disease progression compared to control animals, with 14% of animals from the FC-10696 treated group surviving a lethal MARV challenge up to 21 days post-infection. These findings represent the first proof-of-concept efficacy study for a novel host-oriented antiviral that has the potential for broad-spectrum activity against other PPxY containing viruses such as EBOV and Lassa virus (LASV), and provides proof-of-principle for further development of these first-in-class compounds targeting viral L-domain/host interactions as effective countermeasures to reduce virus budding and dissemination.

Results:

ADME, PK, and anti-budding data for compound FC-10696.. We improved drug disposition properties of a previously described series (26) to generate a novel small molecule FC-10696, a compound with vastly improved overall ADME and PK properties (Table 1), and with robust anti-budding activity against mVP40 VLPs (Table 1 and Fig. 1). Indeed, results from a representative mVP40 VLP budding assay highlight the dose-dependent decrease in mVP40 VLP egress from HEK239T cells treated with increasing concentrations of FC-10696 (Fig. 1, lanes 3-6) compared to that from a vehicle (DMSO) alone treated control (Fig. 1, lane 1). Previously described active compound **1** (FC-4005) at 1.0μM served as a positive control (Fig. 1, lane 2) (26). As expected, equivalent amounts of mVP40 were detected in cell lysates from all samples (Fig. 1, Cells, lanes 1-6). Quantitative results from at least three independent mVP40 VLP budding assays in the presence of 0.3μM or 0.1μM concentration of FC-10696 revealed an average of 91% and 82% inhibition of mVP40 VLP egress, respectively compared to DMSO alone (Table 1).

We evaluated compound FC-10696 in a single dose mouse PK experiment under IP administration (Table 1). FC-10696 displayed excellent blood levels and good metabolic stability (Table 1). Indeed, FC-10696 was

deemed suitable for live virus and mouse efficacy experiments, as it showed good stability to mouse and human liver microsomes and did not inhibit cytochrome P450 3A4 at concentrations up to 33uM, thus showing low risk for drug/drug interactions. In sum, FC-10696 had overall superior ADME and PK properties, as well as robust anti-budding activity in an mVP40 VLP budding assay.

Compound FC-10696 inhibits egress and spread of live MARV in cell culture. To assess safety of FC-10696, we first assessed its cytotoxicity in a HeLa cell line, routinely used in anti-filoviral screens, and human monocyte-derived macrophages (MDMs), the initial targets of filovirus infection in the host (31, 32). Cells treated with 2-fold dilutions of FC-10696 or DMSO as a control were assessed for the number of metabolically active cells after 48 or 72 h. The CC_{50} value, the concentration that reduced the cell viability by 50% when compared to untreated control, showed that the compound was more cytotoxic to HeLa cells than to MDMs (Table 2 and Fig. 2A). Assessment of efficacy revealed that FC-10696 efficiently inhibited live MARV replication and egress in both cell types (Figs. 2B-D). Notably, the half maximal inhibitor concentration, IC_{50}, value in the virion egress assay was at nanomolar concentrations, and the selectivity index, SI_{50}, calculated as CC_{50}/IC_{50}, was $\geq$10, signifying antiviral potency and selectivity of these compounds against this virus.

Compound FC-10696 shows efficacy in a mouse challenge model of MARV infection. To evaluate antiviral potential of FC-10696 compound *in vivo*, BALB/cJ mice challenged intraperitoneally (IP) with 1,000 plaque-forming units (PFU) of mouse-adapted MARV were IP-dosed with a formulation containing the compound twice daily (BID) for 10 consecutive days, starting 6 h post-challenge. BALB/cJ mice are highly susceptible to infection with mouse-adapted MARV, developing disease symptoms and high viremia approximately three days post-infection, and succumbing to the disease by day 6 (33). We found that treatment with 20 mg/kg delayed the onset of mortality ($p=0.0182$; Fig. 3A), weight loss (Fig. 3B), and virus load in serum ($p=0.0255$; Fig. 3D). Importantly, the compound was well-tolerated in mice at the 20 mg/kg, showing that animals

developed only transient treatment-associated toxicity (Fig. 4). Our results demonstrate the proof-of-concept *in vivo* activity for FC-10696 compound against MARV infection.

Discussion:

The identification of host-oriented antiviral compounds represents a promising strategy to develop effective, broad-spectrum therapeutics capable of targeting a wide array of emerging pathogens, which may lead to a paradigm shift in the search for new antivirals (25-28, 34-43). MARV and other filoviruses continue to emerge and cause outbreaks of severe hemorrhagic fever largely originating in Africa, but with the potential to spread globally as observed with the EBOV outbreak in 2014-2015. Here, we report on our continued efforts to develop compounds targeting viral PPxY-mediated host interactions as a novel class of antiviral therapeutics. We demonstrate the antiviral efficacy of novel compound FC-10696 in an in vitro and in vivo model of MARV infection.

Extensive SAR led to the identification of compound FC-10696 , which possesses excellent overall ADME and PK properties. FC-10696 exhibited potent activity at the BSL-2 level in blocking egress of mVP40 VLPs at low nanomolar concentrations in repeated experiments, and in disrupting a PPxY/WW-domain mediated interaction between mVP40 and human E3 ubiquitin ligase Nedd4 as determined using a bimolecular complementation (BiMC) approach (data not shown). FC-10696 was then moved into the BSL-4 laboratory where it was assessed for cytotoxicity in both Hela cells and hMDMs, as well as in BALB/c mice. After obtaining a satisfactory cytotoxicity profile and CC_{50} values, we went on to demonstrate that FC-10696 significantly inhibited MARV egress and spread from primary human macrophages compared to controls. Most intriguingly, we went on to show that treatment of mice with 20 mg/kg twice daily for 10 days delayed the onset of mortality ($p=0.0182$), weight loss, and virus load in serum ($p=0.0255$), thus providing strong support for this class of compounds for further development into potent antivirals against filoviruses and possibly other viruses that utilize PPxY L-domain motifs for productive infection. These findings represent the first proof-of-concept in vivo activity for our lead host-oriented PPxY inhibitor.

Studies are currently underway to assess compound FC-10696 and similar analogs for antiviral potency against related PPxY-containing viruses including EBOV and LASV. Indeed, preliminary findings indicate that FC-10696 can block egress and spread of both eVP40 VLPs and authentic EBOV in vitro; albeit less efficiently than MARV. This may be due to the presence of a second overlapping PTAP L-domain motif with the EBOV VP40 protein that in addition to the PPxY motif, can also function in promoting efficient egress and spread of EBOV, which is in contrast to the single isolated PPxY motif present in the MARV VP40 protein (24). As such, one could envision the use of a PPxY-mediated inhibitor such as FC-10696 in combination with a PTAP-mediated inhibitor, or a viral entry inhibitor for example as part of an antiviral cocktail strategy targeting multiple stages of the virus lifecycle for maximal effect (27, 30, 44-46). Our long term goal is to develop these compounds alone or in combination primarily for individuals in high risk situations including those in the military, health care workers, and first-line responders during an outbreak or epidemic. Additional studies are still needed to precisely identify the mechanism of action and drug interaction site, as well as additional studies to assess cytotoxicity and potential effects on the host in a wider array of cell types.

Materials and Methods:

Cells, Plasmids, and Virus Strain

HEK293T, HeLa, and Vero cells were maintained in Dulbecco's modified Eagle's medium (DMEM) supplemented with 10% fetal bovine serum, penicillin (100U/ml)/streptomycin (100µg/ml), and the cells were grown at 37°C in a humidified 5% CO_2 incubator. Flag-tagged mVP40 plasmid was kindly provided by S. Becker (Institut für Virologie, Marburg, Germany). Monocyte-derived human macrophages (MDMs) were isolated as described previously (47, 48). Peripheral blood was collected from healthy donors according to University of Texas Health approved IRB protocol 20180013HU. Heparinized blood was over-layed onto a Ficoll-Paque cushion (GE Heathcare, Uppsala, Sweden) to isolate peripheral blood mononuclear cells (PBMCs). PBMCs were cultured in suspension in RPMI medium supplemented with 20% autologous serum

for 6 days at 37°C in a humidified 5% CO_2 incubator to differentiate monocytes into macrophages. All experiments with live MARV were performed in the biosafety level 4 (BSL-4) laboratory at the Texas Biomedical Research Institute (TBRI, San Antonio, TX). MARV strain Musoke (NCBI accession number NC_001608) was obtained from the virus repository at the Texas Biomedical Research Institute. Mouse-adapted MARV strain Angola (NCBI accession number KM_261523) was generously provided by the National Microbiology Laboratory, Public Health Agency of Canada. Virus stocks were generated and characterized as described previously (33, 49).

ADME and PK data

Human and mouse liver microsome stability studies and pharmacokinetic studies in mice were performed at Alliance Pharma, Inc. (17 Lee Boulevard, Malven, PA 19355). PK parameters from the PK study were calculated by M. Saporito.

Human and mouse liver microsome stability

FC-10696, at a concentration of 0.5 uM was incubated with 0.5 mg/mL of liver microsomes (mouse or human) and an NADPH-regenerating system (cofactor solution) in potassium phosphate buffer (pH 7.4). At 0, 5, 15, 30, and 45 minutes, an aliquot was taken, and reactions were quenched with an acetonitrile solution containing an internal standard. Midazolam was run as a reference standard. Additionally, controls were measured that do not contain the cofactor solution. Following completion of the experiment, samples were analyzed by LC-MS/MS. Results were reported as peak area ratios of each analyte to internal standard. The intrinsic clearance {CL_{int}) was determined from the first-order elimination constant by nonlinear regression.

Pharmacokinetics in mice

A single-dose study was conducted in adult BalbC male mice of weight range 20-26 g each. Groups of six animals were administered an intravenous 2 mg/Kg (IV) dose or an intraperitoneal 10 mg/Kg (IP) dose of FC-10696 both administered as a soluble 5% DMSO/20% Kleptose aqueous formulation. Plasma samples (n= 3 per timepoint) were collected from study animals at 5, 15, 30 min; 1, 2, 6 hrs for the IV dose and 15,

99 30 min; 1, 2, 6 hrs for the IP dose. Collected samples were analyzed by LC-MS/MS. PK parameters were
00 calculated using Prism Graphpad.

01 VLP Budding Assays

02 MARV VP40 VLP budding assays in HEK293T cells were described previously (2). For VLP budding,
03 HEK293T cells were transfected with 0.5µg of mVP40, and cells were treated with DMSO alone or the
04 indicated concentration of inhibitor for 24 hours post transfection. The mVP40 protein in cell extracts and
05 VLPs was detected by SDS-PAGE and Western blotting and quantified using NIH Image-J software. Anti-
06 flag monoclonal antibody was used to detect flag-tagged mVP40.

07 MARV Egress and Spread Assays

08 HeLa cells or MDMs were plated into wells of a 96-well plate at $2x10^4$ or $5x10^4$ cells/well, respectively, to
09 determine cytotoxic and antiviral properties of FC-10696. All treatments were performed in triplicate. In
10 cytotoxicity assays, cells were left untreated or treated with the compound at eleven 2-fold serially diluted
11 concentrations or DMSO (solvent) for 48 or 72 h. The number of metabolically active cells was determined
12 using a CellTiter-Glo kit. The concentration that reduced the cell viability by 50% when compared to
13 untreated control, CC_{50} value, at each time point was determined using non-linear regression analysis using
14 GraphPad 8 software to select a non-toxic concentration range for antiviral tests.

15 In virus tests, HeLa cells or MDMs were challenged with MARV at multiplicity of infection (MOI) of
16 0.01 for 1 h to allow binding, then washed and incubated with new medium containing seven 2-fold serially
17 diluted concentration of the compounds, equal concentrations of DMSO, or no treatment, for 48 or 72 h. To
18 assess virus egress, cell supernatants were titrated on Vero cells for 24 h. Infected cells were detected by
19 treatment with MARV VLP antibody (IBT Bioservices, Rockville, MD), and nuclei by staining with Hoechst
20 dye (Thermo Fisher Scientific, Waltham, MA). Samples were photographed using a Nikon automated system
21 (Nikon, Tokyo, Japan) and analyzed by CellProfiler software (Broad Institute, Cambridge, MA) to quantify
22 virus spread and egress. Infection efficiency in treated samples was determined as a ratio of infected cells
23 and nuclei and reported relative to mock. The half maximal inhibitor concentration, IC_{50}, value for virus

spread and egress for each time point was determined by non-linear regression analysis. The selectivity index, SI_{50}, determined as CC_{50}/IC_{50}, was used to assess antiviral potential of the compounds.

Animals

Wild-type 4-week old female BALB/cJ mice were obtained from The Jackson Laboratory (Bar Harbor, ME). The mouse studies were conducted in strict adherence to the Animal Welfare Act and the Guide for the Care and Use of Laboratory Animals of the National Institutes of Health (NIH). The TBRI animal assurance welfare number is D16-00048 (A3082-01) under file with the NIH. All mouse procedures were approved by the TBRI Institutional Animal Care and Use Committee (IACUC) which oversees the administration of the IACUC protocols. The mouse studies were performed as outlined in the IACUC protocol #1708MU.

In Vivo Efficacy Studies

To assess toxicity of FC-10696 treatment in mice, the compound was resuspended in 30%PEG400/ 2%DMSO/14%kleptose HPB parenteral grade (Roquette, Lestrem, France) formulation at two different concentrations, 20 and 4 mg/kg, and administered to groups of five 4-week old female BALB/cJ mice twice daily (BID) via the intraperitoneal route (IP) for a period of 10 days. Animals were monitored daily for signs of treatment-associated toxicity: weight loss, rough hair coat, discharge from eyes and nose, diarrhea, decreased food intake and activity, and mortality. Clinical scores for each group were recorded as a sum of all observations in the group.

To assess antiviral potential of FC-10696 treatment in a mouse model of MARV disease, three groups of ten 4-week old female BALB/cJ mice were challenged with 1,000 plaque-forming units (PFUs, as determined on Vero cells) of mouse-adapted MARV by the IP route. IP dosing by vehicle or FC-10696 at either 20 or 10 mg/kg started 6 h post-challenge and continued BID for 10 consecutive days. Animals were observed at least twice daily for signs of viral disease (ruffled hair coat, hunch back, inappetence, weight loss, and decreased movement) and mortality for 21 days post-challenge. Group clinical scores were recorded as the sum of all clinical observations for the group. If a clinical score of $\geq$12 was recorded for an animal, it was considered terminally ill and euthanized. Three animals from each group were euthanized on

day 3 post-challenge to collect blood to determine virus titer by a plaque assay. The remaining 7 mice/group were used to determine animal survival.

Acknowledgments:

Funding was provided in part by National Institutes of Health grants AI138052 and AI138630 to RNH, AI129890 to BDF, T32-AI070077 to ASM, and an Innovator Award from The Wellcome Trust to MSS. The funders had no role in study design, data collection and analysis, decision to publish, or preparation of the manuscript.

Conflict of Interest:

I have read the journal's policy and the authors of this manuscript have the following competing interests: RNH and BDF are co-founders of Intervir, LLC.

Figure Legends:

Fig. 1. FC-10696 inhibits budding of mVP40 VLPs in a dose-dependent manner. HEK293T cells were transfected with mVP40 in the presence of DMSO alone, compound 1, or the indicated concentrations of compound FC-10696. mVP40 was detected in cell lysates and VLPs by Western blotting, and mVP40 levels in VLPs were quantified using NIH Image-J software (shown in parentheses).

Fig. 2. FC-10696 inhibits egress and spread of live MARV from infected human MDMs. **(A)** MDMs were left untreated or treated with FC-10696 at 11 2-fold serially diluted concentrations or DMSO for 48 or 72 h in triplicate. The number of metabolically active cells was determined using a CellTiter-Glo kit. The relative light unit (RLUs) value for each concentration is an average ± standard deviation of 3 replicates. **(B)** MDMs were challenged with MARV for 1 h, then washed and incubated with new medium containing 7 2-fold serially diluted concentration of the compounds, equal concentrations of DMSO, or no treatment, for 48 or

72 h. Subsequently, cells were stained with anti-VLP antibody and Hoechst dye, and photographed. Numbers of nuclei and infected cells were counted using CellProfiler software. The relative infection efficiencies, determined by dividing the number of infected cells by the number of nuclei, are reported relative to the infection efficiency in untreated cells and are averages ± standard deviations of 3 replicates. **(C)** To assess virus egress from FC-10696-treated MDMs, cell supernatants were titrated on Vero cells for 24 h. The samples were then treated with anti-VLP antibody and Hoechst dye. Samples were imaged and analyzed as above. **(D)** Supernatants of MDMs challenged with MARV and treated as indicated for 72 h were titrated on Vero cells. Samples were treated with anti-VLP antibody to detect infected cells (green) and Hoechst dye to detect nuclei (blue) and imaged using a Nikon imaging system. The bar in each image is 100 µm.

Fig. 3. In vivo efficacy of FC-10696 in a mouse model of MARV disease. Three groups of 10 4-week old female BALB/cJ mice were challenged with 1,000 PFUs of mouse-adapted MARV. IP dosing by vehicle or FC-10696 at either 20 or 10 mg/kg started 6 h post-challenge and continued BID for 10 consecutive days. Animals were observed daily for mortality **(A)**, weight loss **(B)**, and clinical signs of disease **(C)** for 21 days post-infection. Clinical scores for each group were recorded as a sum of all observations in the group, and if a score of ≥12 was recorded for an individual animal, it was considered terminally ill and euthanized. On day 3 post-challenge, 3 animals/group were euthanized to collect serum for virus load assessment by the neutral red plaque assay **(D)**. The remaining 7 mice/group were used to determine animal survival. Viral burden was analyzed using a Student *t*-test or one-way ANOVA Tukey's test, and survival analysis was performed using a Log-rank (Mantel-Cox) test, with $p \leq 0.05$ considered significant in all analyses.

Fig. 4. *In vivo* toxicity data for FC-10696. FC-10696 was resuspended in 30%PEG400/ 2%DMSO/14%kleptose HPB parenteral grade formulation at two different concentrations, 20 and 4 mg/kg, and administered to groups of five 4-week old female BALB/cJ mice BID via the IP route for a period of 10 days. Animals were monitored daily for signs of treatment-associated toxicity: weight loss **(A)**; rough hair

coat, discharge from eyes and nose, diarrhea, decreased food intake and activity **(B)**; and mortality. Clinical scores for each group were recorded as a sum of all observations in the group.

References:

1. **Feldmann H, Klenk HD.** 1996. Marburg and Ebola viruses. Adv Virus Res **47:**1-52.

2. **Han Z, Dash S, Sagum CA, Ruthel G, Jaladanki CK, Berry CT, Schwoerer MP, Harty NM, Freedman BD, Bedford MT, Fan H, Sidhu SS, Sudol M, Shtanko O, Harty RN.** 2020. Modular mimicry and engagement of the Hippo pathway by Marburg virus VP40: Implications for filovirus biology and budding. PLoS Pathog **16:**e1008231.

3. **Harty RN.** 2018. Hemorrhagic Fever Virus Budding Studies. Methods Mol Biol **1604:**209-215.

4. **Wijesinghe KJ, Urata S, Bhattarai N, Kooijman EE, Gerstman BS, Chapagain PP, Li S, Stahelin RV.** 2017. Detection of lipid-induced structural changes of the Marburg virus matrix protein VP40 using hydrogen/deuterium exchange-mass spectrometry. J Biol Chem **292:**6108-6122.

5. **Liang J, Sagum CA, Bedford MT, Sidhu SS, Sudol M, Han Z, Harty RN.** 2017. Chaperone-Mediated Autophagy Protein BAG3 Negatively Regulates Ebola and Marburg VP40-Mediated Egress. PLoS Pathog **13:**e1006132.

6. **Oda S, Noda T, Wijesinghe KJ, Halfmann P, Bornholdt ZA, Abelson DM, Armbrust T, Stahelin RV, Kawaoka Y, Saphire EO.** 2016. Crystal Structure of Marburg Virus VP40 Reveals a Broad, Basic Patch for Matrix Assembly and a Requirement of the N-Terminal Domain for Immunosuppression. J Virol **90:**1839-1848.

7. **Urata S, Yasuda J.** 2010. Regulation of Marburg virus (MARV) budding by Nedd4.1: a different WW domain of Nedd4.1 is critical for binding to MARV and Ebola virus VP40. J Gen Virol **91:**228-234.

8. **Liu Y, Cocka L, Okumura A, Zhang YA, Sunyer JO, Harty RN.** 2010. Conserved motifs within Ebola and Marburg virus VP40 proteins are important for stability, localization, and subsequent budding of virus-like particles. J Virol **84:**2294-2303.

9. **Urata S, Noda T, Kawaoka Y, Morikawa S, Yokosawa H, Yasuda J.** 2007. Interaction of Tsg101 with Marburg virus VP40 depends on the PPPY motif, but not the PT/SAP motif as in the case of Ebola virus, and Tsg101 plays a critical role in the budding of Marburg virus-like particles induced by VP40, NP, and GP. J Virol **81:**4895-4899.

10. **Kolesnikova L, Bohil AB, Cheney RE, Becker S.** 2007. Budding of Marburgvirus is associated with filopodia. Cell Microbiol **9:**939-951.

11. **Hartlieb B, Weissenhorn W.** 2006. Filovirus assembly and budding. Virology **344:**64-70.

12. **Swenson DL, Warfield KL, Kuehl K, Larsen T, Hevey MC, Schmaljohn A, Bavari S, Aman MJ.** 2004. Generation of Marburg virus-like particles by co-expression of glycoprotein and matrix protein. FEMS Immunol Med Microbiol **40:**27-31.

13. **Kolesnikova L, Berghofer B, Bamberg S, Becker S.** 2004. Multivesicular bodies as a platform for formation of the Marburg virus envelope. J Virol **78:**12277-12287.

14. **Jasenosky LD, Kawaoka Y.** 2004. Filovirus budding. Virus Res **106:**181-188.

15. **Kolesnikova L, Bugany H, Klenk HD, Becker S.** 2002. VP40, the matrix protein of Marburg virus, is associated with membranes of the late endosomal compartment. J Virol **76:**1825-1838.

16. **Harty RN, Brown ME, Wang G, Huibregtse J, Hayes FP.** 2000. A PPxY motif within the VP40 protein of Ebola virus interacts physically and functionally with a ubiquitin ligase: implications for filovirus budding. Proc Natl Acad Sci U S A **97:**13871-13876.

17. **Han Z, Sagum CA, Bedford MT, Sidhu SS, Sudol M, Harty RN.** 2016. ITCH E3 Ubiquitin Ligase Interacts with Ebola Virus VP40 To Regulate Budding. J Virol **90:**9163-9171.

18. **Liu Y, Lee MS, Olson MA, Harty RN.** 2011. Bimolecular Complementation to Visualize Filovirus VP40-Host Complexes in Live Mammalian Cells: Toward the Identification of Budding Inhibitors. Adv Virol **2011**.

19. **Han Z, Sagum CA, Takizawa F, Ruthel G, Berry CT, Kong J, Sunyer JO, Freedman BD, Bedford MT, Sidhu SS, Sudol M, Harty RN.** 2017. Ubiquitin Ligase WWP1 Interacts with Ebola Virus VP40 To Regulate Egress. J Virol **91**.

20. **Okumura A, Pitha PM, Harty RN.** 2008. ISG15 inhibits Ebola VP40 VLP budding in an L-domain-dependent manner by blocking Nedd4 ligase activity. Proc Natl Acad Sci U S A **105:**3974-3979.

21. **Martin-Serrano J, Perez-Caballero D, Bieniasz PD.** 2004. Context-dependent effects of L domains and ubiquitination on viral budding. J Virol **78:**5554-5563.

22. **Yasuda J, Nakao M, Kawaoka Y, Shida H.** 2003. Nedd4 regulates egress of Ebola virus-like particles from host cells. J Virol **77:**9987-9992.

23. **Timmins J, Schoehn G, Ricard-Blum S, Scianimanico S, Vernet T, Ruigrok RW, Weissenhorn W.** 2003. Ebola virus matrix protein VP40 interaction with human cellular factors Tsg101 and Nedd4. J Mol Biol **326:**493-502.

24. **Licata JM, Simpson-Holley M, Wright NT, Han Z, Paragas J, Harty RN.** 2003. Overlapping motifs (PTAP and PPEY) within the Ebola virus VP40 protein function independently as late budding domains: involvement of host proteins TSG101 and VPS-4. J Virol **77:**1812-1819.

25. **Shepley-McTaggart A, Fan H, Sudol M, Harty RN.** 2020. Viruses go modular. J Biol Chem doi:10.1074/jbc.REV119.012414.

26. **Loughran HM, Han Z, Wrobel JE, Decker SE, Ruthel G, Freedman BD, Harty RN, Reitz AB.** 2016. Quinoxaline-based inhibitors of Ebola and Marburg VP40 egress. Bioorg Med Chem Lett **26:**3429-3435.

27. **Lu J, Han Z, Liu Y, Liu W, Lee MS, Olson MA, Ruthel G, Freedman BD, Harty RN.** 2014. A host-oriented inhibitor of Junin Argentine hemorrhagic fever virus egress. J Virol **88:**4736-4743.

28. **Han Z, Lu J, Liu Y, Davis B, Lee MS, Olson MA, Ruthel G, Freedman BD, Schnell MJ, Wrobel JE, Reitz AB, Harty RN.** 2014. Small-molecule probes targeting the viral PPxY-host Nedd4 interface block egress of a broad range of RNA viruses. J Virol **88:**7294-7306.

29. **Harty RN.** 2009. No exit: targeting the budding process to inhibit filovirus replication. Antiviral Res **81:**189-197.

30. **Perez M, Craven RC, de la Torre JC.** 2003. The small RING finger protein Z drives arenavirus budding: implications for antiviral strategies. Proc Natl Acad Sci U S A **100:**12978-12983.

31. **Bray M, Geisbert TW.** 2005. Ebola virus: The role of macrophages and dendritic cells in the pathogenesis of Ebola hemorrhagic fever. International Journal of Biochemistry & Cell Biology **37:**1560-1566.

32. **Hensley LE, Alves DA, Geisbert JB, Fritz EA, Reed C, Larsen T, Geisbert TW.** 2011. Pathogenesis of Marburg Hemorrhagic Fever in Cynomolgus Macaques. Journal of Infectious Diseases **204:**S1021-S1031.

33. **Qiu XG, Wong G, Audet J, Cutts T, Niu YL, Booth S, Kobinger GP.** 2014. Establishment and Characterization of a Lethal Mouse Model for the Angola Strain of Marburg Virus. Journal of Virology **88:**12703-12714.

34. **Liu Y, Harty RN.** 2010. Viral and host proteins that modulate filovirus budding. Future Virol **5:**481-491.

35. **Iglesias-Bexiga M, Palencia A, Corbi-Verge C, Martin-Malpartida P, Blanco FJ, Macias MJ, Cobos ES, Luque I.** 2019. Binding site plasticity in viral PPxY Late domain recognition by the third WW domain of human NEDD4. Scientific Reports **9**.

36. **de Chassey B, Meyniel-Schicklin L, Vonderscher J, Andre P, Lotteau V.** 2014. Virus-host interactomics: new insights and opportunities for antiviral drug discovery. Genome Medicine **6**.

94 37. **Heaton SM.** 2019. Harnessing host-virus evolution in antiviral therapy and immunotherapy. Clinical
95 & Translational Immunology **8**.
96 38. **Sui BQ, Bamba D, Weng K, Ung H, Chang SJ, Van Dyke J, Goldblatt M, Duan R, Kinch MS,**
97 **Li WB.** 2009. The use of Random Homozygous Gene Perturbation to identify novel host-oriented
98 targets for influenza. Virology **387:**473-481.
99 39. **Kinch MS, Yunus AS, Lear C, Mao HW, Chen HS, Fesseha Z, Luo GX, Nelson EA, Li LM,**
00 **Huang ZH, Murray M, Ellis WY, Hensley L, Christopher-Hennings J, Olinger GG, Goldblatt**
01 **M.** 2009. FGI-104: a broad-spectrum small molecule inhibitor of viral infection. American Journal of
02 Translational Research **1:**87-98.
03 40. **Liu Y, Harty RN.** 2010. Viral and host proteins that modulate filovirus budding. Future Virology
04 **5:**481-491.
05 41. **Lu JH, Han ZY, Liu YL, Liu WB, Lee MS, Olson MA, Ruthel G, Freedman BD, Harty RN.**
06 2014. A Host-Oriented Inhibitor of Junin Argentine Hemorrhagic Fever Virus Egress. Journal of
07 Virology **88:**4736-4743.
08 42. **Han ZY, Madara JJ, Herbert A, Prugar LI, Ruthel G, Lu JH, Liu YL, Liu WB, Liu XH,**
09 **Wrobel JE, Reitz AB, Dye JM, Harty RN, Freedman BD.** 2015. Calcium Regulation of
10 Hemorrhagic Fever Virus Budding: Mechanistic Implications for Host-Oriented Therapeutic
11 Intervention. Plos Pathogens **11**.
12 43. **Mao HW, Chen HS, Fesseha Z, Chang SJ, Ung-Medoff H, Van Dyke J, Kohli M, Li WB,**
13 **Goldblatt M, Kinch MS.** 2009. Identification of novel host-oriented targets for Human
14 Immunodeficiency Virus type 1 using Random Homozygous Gene Perturbation. Virology Journal **6**.
15 44. **Palencia A, Martinez JC, Mateo PL, Luque I, Camara-Artigas A.** 2006. Structure of human
16 TSG101 UEV domain. Acta Crystallogr D Biol Crystallogr **62:**458-464.
17 45. **Urata S, Noda T, Kawaoka Y, Yokosawa H, Yasuda J.** 2006. Cellular factors required for Lassa
18 virus budding. J Virol **80:**4191-4195.

46. **Capul AA, de la Torre JC.** 2008. A cell-based luciferase assay amenable to high-throughput screening of inhibitors of arenavirus budding. Virology **382:**107-114.

47. **Schlesinger LS.** 1993. Macrophage Phagocytosis of Virulent but Not Attenuated Strains of Mycobacterium-Tuberculosis Is Mediated by Mannose Receptors in Addition to Complement Receptors. Journal of Immunology **150:**2920-2930.

48. **Rogers KJ, Shtanko O, Stunz LL, Mallinger LN, Arkee T, Schmidt ME, Bohan D, Brunton B, White JM, Varga SM, Butler NS, Bishop GA, Maury W.** 2020. Frontline Science: CD40 signaling restricts RNA virus replication in M phi s, leading to rapid innate immune control of acute virus infection. Journal of Leukocyte Biology doi:10.1002/Jlb.4hi0420-285rr.

49. **Shtanko O, Sakurai Y, Reyes AN, Noel R, Cintrat JC, Gillet D, Barbier J, Davey RA.** 2018. Retro-2 and its dihydroquinazolinone derivatives inhibit filovirus infection. Antiviral Res **149:**154-163.

Table 1. In vitro Marburg Egress, ADME and PK data

FC#	Marburg Egress Assay[a]					MW	MLM[b] stability	HLM[c] stability	Mouse PK, IP administration[d]			
	1.0 uM	0.5 uM	0.3 uM	0.1 uM	0.03 uM		t1/2 (min)	t1/2 (min)	Cmax (ng/ml)	AUC (ng x ml/hr)	$t_{1/2}$ (hrs)	IP Bioavail-bility (%)
FC-10696	*99*	*94*	*91*	*86*	*0*	*357.5*	*76.9*	*1670*	*253*	*1378*	*1.5*	*42*

[a]% Reduction of Marburg VLP at listed compound conc, VLP = virus like particle, in HEK293T cell line, with positive control FC-4005(26) run at 1 uM (~90% ± 10%). [b]MLM mouse liver microsome. [c]HLM human liver microsome. [d]BalbC mice administered one time 10 mg/kg of drug with plasma collection time points of 0.25, 0.5, 1, 2, and 6 hr. IP Bioavailbility is the ratio of IP AUC to IV AUC x 100. IV PK parameters are not shown.

Han et al.
Fig. 1

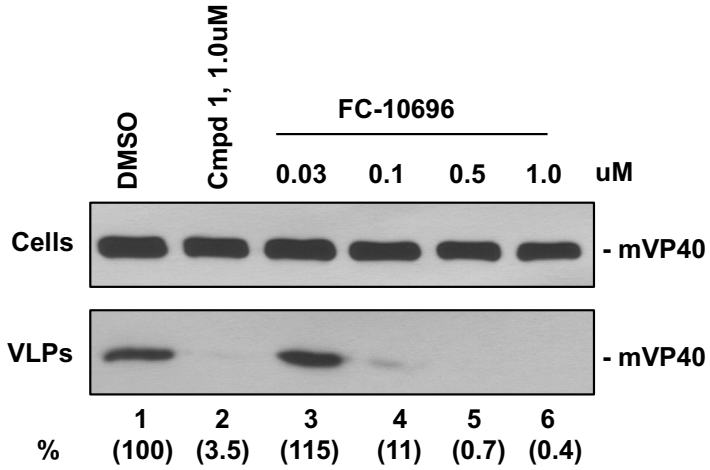

Table 2. FC-10696 IC_{50} and SI_{50} values (in µm) for live MARV egress at 48 h.

Cell type	CC_{50}	IC_{50} egress	SI_{50} egress
HeLa	0.49	0.042	11.7
Human macrophages	4.8	0.18	26.7

Cytotoxic properties of FC-10696 were tested in either HeLa cell line or human macrophages using CellTiter-Glo kit 48 or 72 h after treatment to select non-toxic concentration range for antiviral tests. In the virus tests, cells were challenged with MARV at MOI=0.01 for 1 h, then incubated with new medium containing serially diluted concentrations of the FC-10696. To assess virus egress, cell supernatants were titrated on Vero cells. Infected cells were detected by staining with anti-MARV VLP antibody, and nuclei were stained with Hoechst dye. Samples were subsequently imaged and analyzed. The concentration that reduced cell viability by 50% (CC_{50}) and the half maximal inhibitor concentration (IC_{50}) for virus egress was determined by non-linear regression analysis. Selectivity index (SI_{50}) was calculated as CC_{50}/IC_{50}. Only data for 48 h time point are shown.

Han et al.,
Fig. 2

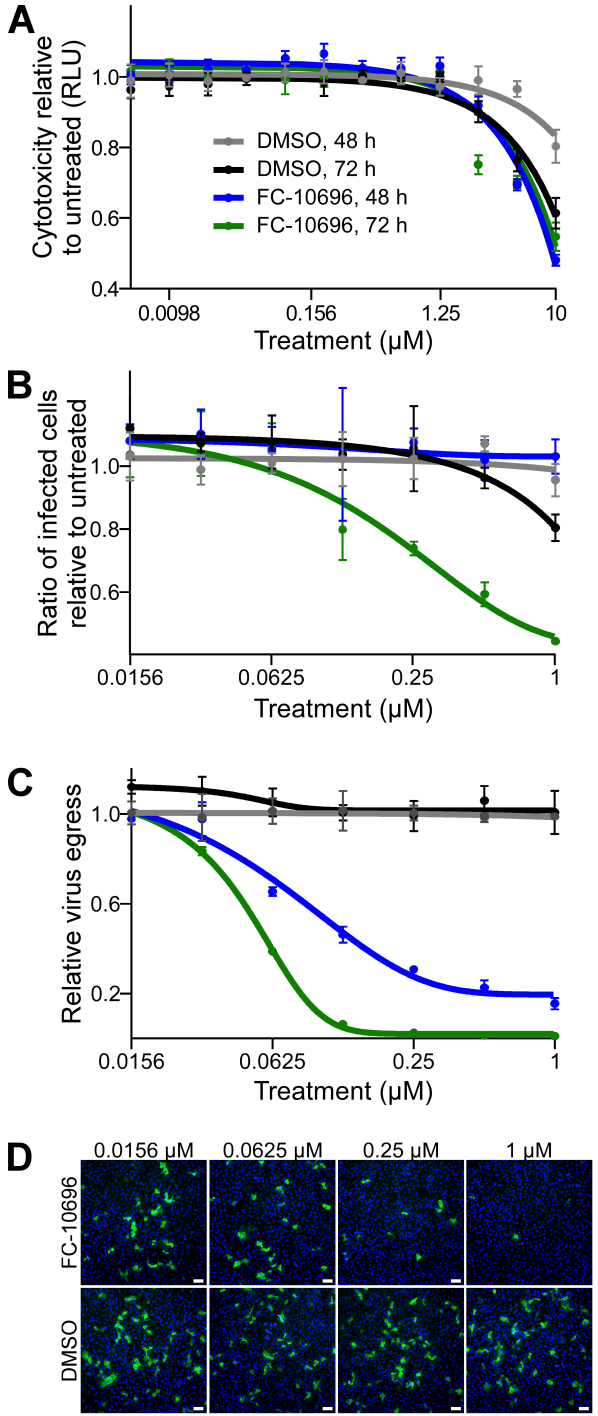

Han et al.,
Fig. 3

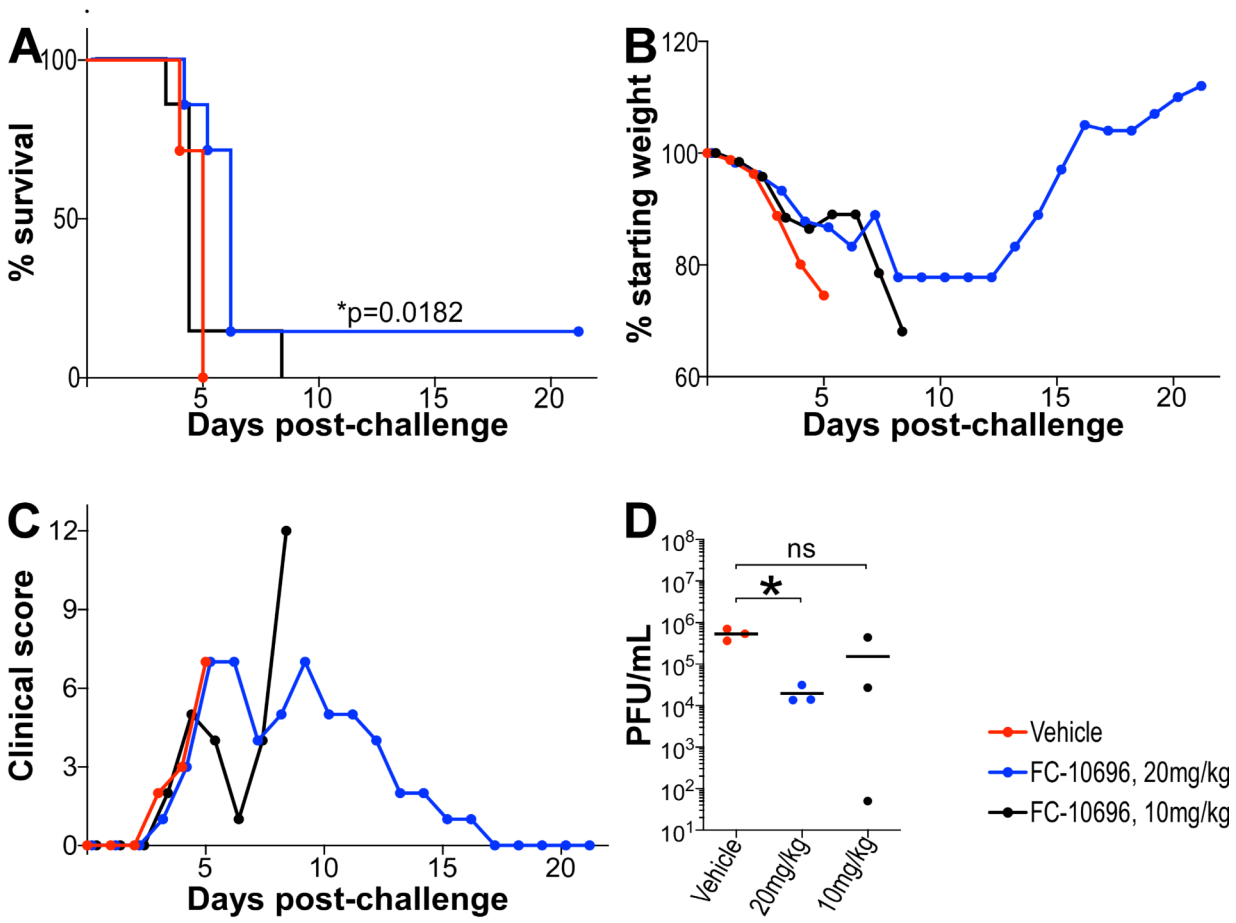

Han et al.,
Fig. 4